AAEC/TM191

AAEC/TM 191

16

AUSTRALIAN ATOMIC ENERGY COMMISSION

RESEARCH ESTABLISHMENT

LUCAS HEIGHTS

INTEGRAL REACTION RATES AND NEUTRON ENERGY SPECTRA IN A WELL MODERATED REACTOR

by

J. W. CONNOLLY

A. ROSE

T. WALL

Issued Sydney, April 1963

AUSTRALIAN ATOMIC ENERGY COMMISSION

RESEARCH ESTABLISHMENT

LUCAS HEIGHTS

INTEGRAL REACTION RATES AND NEUTRON ENERGY SPECTRA IN A WELL MODERATED REACTOR

by

J. W. CONNOLLY

A. ROSE

T. WALL

ABSTRACT

Cadmium ratio measurements in the internal reflector of MOATA have been made with gold, indium, tungsten, manganese, molybdenum, and copper detectors. These measurements have been analysed on the assumption that the neutron spectrum consists of a Maxwellian distribution to which is smoothly joined a $\frac{1}{E}$ slowing down spectrum, cross sections being averaged according to the methods of Westcott. A search through recent literature suggests that the s factors for gold and indium listed by Westcott are in error. If this is accepted then it appears that the measured epithermal spectrum is closely $\frac{1}{E}$ in form for neutron energies between one and six hundred eV.

The corrections to be applied when foils of finite thickness are used in cadmium ratio measurements are discussed, and the spectrum derived from these measurements has been used to calculate reaction rate ratios of copper: indium and copper: gold alloy foils. These ratios have been compared with measured values.

Values of the effective resonance integral of Pt 198 wire detectors have been measured, and from these values an estimate has been made of the infinitely dilute resonance integral of this isotope.

CONTENTS

(continued)

CONTENTS (continued)

1. INTRODUCTION

The use of activation detectors in integral neutron spectrum studies is well established. Such detectors, by virtue of their small size, enable measurements to be made in locations from which it would be difficult to extract a beam for time–of–flight spectrometry. Moreover, the method is much less complex than that required for differential measurements, and although it is not possible to obtain such detailed spectral information as the latter method is capable of yielding, integral measurements can give reliable information on reaction rates of nuclei in a reactor spectrum. Frequently this is of greater interest than knowledge of the detailed shape of the spectrum at a particular location.

In recent years a revival of interest in integral techniques has greatly improved the state of the basic data which must be used in the analysis of integral measurements with activation detectors. Papers by Westcott (1956, 1958, 1960) have dealt with the formulation of correct cross section averaging in well moderated reactor spectra, where time–of–flight measurements have shown the spectrum to consist of a Maxwellian distribution of 'thermal' neutrons of most probable temperature T to which is smoothly joined a $\frac{1}{E}$ spectrum of neutrons slowing down from fission energies.

This paper describes the results of measurements made by activating materials in the graphite internal reflector of MOATA. The work forms part of an attempt to extend the usefulness of such detectors to other than well moderated systems, where the simple two group approach must be replaced by a multigroup formulation of neutron behaviour. It was felt that an investigation using a well moderated system would provide a useful starting point for such an attempt for the following reasons:

(i) A check could be made against the reliability of the nuclear cross section data required for all integral activation measurements.

(ii) The integral measurements could be compared with those obtained from the slow chopper at present installed on MOATA.

(iii) Slowing down theory for well moderated systems is well understood, and forms a useful comparison with results of experiment.

(iv) The specification of the neutron spectrum in MOATA is of interest to other experimenters.

2. EXPERIMENTAL PROCEDURES

2.1 Irradiation

Activation detectors were irradiated in the centre of the central stringer of the graphite internal reflector of MOATA. A full description of this reactor has been given by Marks (1962).

Great care was taken to ensure exact reproducibility of position for all foils during irradiation, and for this purpose the special stringer, shown in Figure 1, was constructed and used. This also enabled the foils to be completely surrounded by graphite without the presence of large air gaps between graphite and foil. All irradiations were monitored by detectors placed in off centre positions of the stringer during each experiment.

For most irradiations discussed here the activation of the foils during reactor start up and shut down was computed using the results of Wall (1963). This is referred to in Section 8.

In the case of reaction rate ratio measurements it was necessary to carry out normalizing irradiations in a pure thermal flux. For this purpose the Low Flux Facility described by Lang and Rose (1963) was used. Measurement of the epithermal index in the irradiation position of the facility yielded the value:

$$r\sqrt{\frac{T}{T_o}} = 0.00036 \pm 0.00009 \quad .$$

Boldeman et al. (1962) have shown that the effective neutron temperature in this assembly is consistent with the physical temperature of the graphite. No appreciable error arose in the work reported here if this spectrum was regarded as purely thermal with a most probable temperature of 295 °K.

2.2 Activation Detectors

The detectors used were Au197, In115, W186, Mo100, Pt198, Cu63, and Mn55. For the reaction rate ratios, alloys of Cu:Au and Cu:In were used. These detectors are fully described in Tables 1 to 8.

The cadmium covers used in the cadmium ratio work were 0.040 inches thick for the plane foils. For the wire detectors the cadmium covers were formed from cadmium tube of wall thickness 0.035 inches and internal diameter 0.030 inches.

2.3 Counting Techniques

All activities induced in the foils were gamma counted to avoid the necessity of making self absorption corrections. The counter consisted of two 2 x 2 inch NaI crystals arranged in nearly 4π geometry. This arrangement was less sensitive to small displacements of the source from the centre of the crystals and had a higher efficiency than if a single small crystal had been used.

A stainless steel foil carrier slid between the two crystals enabling accurate positioning of the samples.

Two potentiometers in parallel across a mains stabilised EHT unit provided the photomultiplier EHT supplies and enabled the gains of the two photomultipliers to be accurately matched.

The output of the two crystals was fed through a non-overloading linear amplifier into a single channel analyser and scaler. Counting bias was chosen after pulse height analysis of the activity, and half life measurements were made to ensure that no "foreign" activity contributed to the activities measured.

The overall stability of this arrangement was frequently checked with a standard Cs137 source. Apart from short term drifts following the switching of the EHT supply from 'stand by' to 'operate', the stability was better than 1 per cent. over most counting periods, which on the average were several hours long. However, an error seemed to be present which was not associated with gain stability and this must be further investigated. It is probable that the cause lay with switching transients when other machinery in the building was brought into operation.

3. EFFECTIVE FLUX AND CROSS SECTION CONVENTION

Time-of-flight measurements on well moderated reactor systems have shown the neutron spectrum to be well approximated by a Maxwellian distribution of velocities to which is smoothly joined a $\frac{1}{E}$ distribution of slowing down neutrons. Using this spectrum model Westcott (1956) developed a formalism for correctly averaging neutron cross-sections in well moderated reactor systems; although this has been discussed elsewhere a summary is included here for convenience.

The assumed spectrum can be written:

$$\phi(E) = n_M \bar{v}_M \left\{ \frac{E}{E_T^2} \exp\left(\frac{-E}{E_T}\right) + \frac{\beta \Delta}{E} \right\} , \qquad (1)$$

where $E_T = kT$ = most probable energy of a Maxwellian of temperature T.

$\bar{v}_M$ = average velocity of the Maxwellian

β relates the epithermal neutron density n_e to the Maxwellian density n_M

Δ is an arbitrary cut-off to the low energy end of the epithermal distribution such that:

$$\Delta = 0 \quad \text{for} \quad E < \mu kT$$

$$\Delta = 1 \quad \text{for} \quad E > \mu kT ,$$

and the nature of this joining function is discussed in more detail below (see Section 3.1).

Equation 1 may be expressed in terms of a velocity distribution since $dE = v\,dv$ implies that

$$v\,\phi(E) = \phi(v) = v\,n(v) ,$$

and thus

$$n(v) = n_M\,\bar{v}_M \left\{ \frac{2\,v^2}{v_T^4} \exp - \left(\frac{v}{v_T}\right)^2 + \frac{2\beta\Delta}{v^2} \right\} .$$

For a Maxwellian distribution

$$\bar{v} = v_T \sqrt{\frac{4}{\pi}} ,$$

and therefore

$$n(v) = \frac{4\,n_M}{\sqrt{\pi}} \left\{ \frac{v^2}{v_T^3} \exp - \left(\frac{v}{v_T}\right)^2 + \frac{v_T}{v^2}\,\beta\Delta \right\} . \qquad (2)$$

The total 'true' flux is then given by integrating this neutron density distribution multiplied by velocity over all velocities, that is,

$$\Phi = \int_0^\infty v\,n(v)\,dv ,$$

and the total neutron density is similarly

$$n = \int_0^\infty n(v)\,dv .$$

Since the mean neutron velocity is

$$\bar{v} = \frac{\int_0^\infty v\,n(v)\,dv}{\int_0^\infty n(v)\,dv} ,$$

it can be seen that

$$\Phi = n\,\bar{v} .$$

There are two objections to using this as a flux definition in a reactor spectrum. First, too much weight (from a reaction rate point of view) is placed on the relatively few high energy epithermal neutrons. Secondly, unless the form and magnitude of the distribution $v\,n(v)$ are known, the definition cannot be used to measure flux experimentally.

In practice the reaction rate of a $\frac{1}{v}$ absorber is measured and used as the basis of the flux definition. Such a detector always measures neutron density, irrespective of the shape of the spectrum. This may be seen by writing the reaction rate of such a detector as:

$$R_{\frac{1}{v}} = \int_0^\infty \sigma(v)\,v\,n(v)\,dv$$

$$= \int_0^\infty \sigma_o\,v_o\,n(v)\,dv$$

$$= n\,v_o\,\sigma_o$$

where σ_o is the value of the cross section at $v_o = 2200$ m/sec.

Flux is then defined as:

$$n\, v_o = \frac{R_{\frac{1}{v}}}{\sigma_o} \quad .$$

For a Maxwellian distribution the true flux can be obtained since

$$v_o = \bar{v} \sqrt{\frac{\pi\, T_o}{4\, T}} \quad .$$

Using $n\, v_o$ as the definition of conventional flux, the effective cross section is then defined as that cross section which, when used with the conventional flux, gives the same reaction rate as is observed when the material is placed in the actual spectrum $\phi(E)$. This effective cross section can be denoted:

$$\hat{\sigma} = \frac{\text{Reaction rate of nuclide in spectrum } \phi(E)}{n\, v_o}$$

$$= \frac{\int_o^\infty \sigma(E)\, \phi(E)\, dE}{v_o \int_o^\infty \frac{\phi(E)}{v}\, dE} \quad .$$

The Maxwellian component of the total cross section is then written:

$$\hat{\sigma}_M = \frac{\int_o^\infty \sigma(v)\, n_M(v)\, dv}{n_M\, v_o}$$

$$= \frac{4}{\sqrt{\pi}\, v_T^3\, v_o} \int_o^\infty v^3 \exp - \left(\frac{v}{v_T}\right)^2 \sigma(v)\, dv \quad ,$$

and if the cross section follows the $\frac{1}{v}$ law then $\hat{\sigma}_M$ reduces to σ_o .

For materials which do not obey this law,

$$\hat{\sigma}_M = g(T)\, \sigma_o \quad ,$$

where

$$g(T) = \frac{4}{\sqrt{\pi}\, v_T^3\, v_o\, \sigma_o} \int_o^\infty v^3 \exp - \left(\frac{v}{v_T}\right)^2 \sigma(v)\, dv$$

$$= \frac{\text{Reaction rate of nuclide in Maxwellian of temperature T}}{\text{2200 m/sec reaction rate}} \quad .$$

Thus $g(T)\sigma_o$ is a conventional $\frac{1}{v}$ cross section which would give the same reaction rate in the Maxwellian as does the actual cross section $\sigma(v)$. The function g(T) will thus be a useful indicator of neutron temperature if the nuclide possesses pronounced resonances in the thermal region.

For the epithermal component of the cross section,

$$\hat{\sigma}_e = \frac{\frac{4\, n_M}{\sqrt{\pi}} \int_{\sqrt{2\mu kT}}^\infty \sigma(v)\, \frac{v_T}{v^2}\, .\, v\, .\, \beta\, .\, \Delta\, .\, dv}{n_e\, v_o}$$

and for

$$\sigma(v) = \sigma_o\, \frac{v_o}{v} \quad ,$$

$$\hat{\sigma}_e = \frac{n_M}{n_e}\, \frac{4}{\sqrt{\pi\mu}}\, \beta\, \sigma_o = \sigma_o \quad ,$$

where β is defined:

$$\beta = \frac{n_e}{n_M}\frac{\sqrt{\pi\mu}}{4} = \frac{n_e}{n_M}\frac{1}{b} .$$

Nearly all nuclides have pronounced resonances in the epithermal region and the important case of non-$\frac{1}{v}$ cross section in this region is now considered.

The epithermal reaction rate is:

$$R_e = \int_{\sqrt{2\mu kT}}^{\infty} \sigma(v)\, n_e(v)\, dv$$

$$= \frac{4\, n_M\, v_T}{\sqrt{\pi}} \cdot \beta \int_{\sqrt{2\mu kT}}^{\infty} \sigma(v)\, \frac{dv}{v}$$

$$= 4\, n_M\, v_T\, \beta\, \frac{\Sigma}{2\sqrt{\pi}}$$

where the resonance integral is defined by:

$$\Sigma = \int_{\mu kT}^{\infty} \sigma(E)\, \frac{d(E)}{E}$$

$$= 2 \int_{\sqrt{2\mu kT}}^{\infty} \sigma(v)\, \frac{dv}{v} .$$

It is convenient to express the resonance integral as the sum of the $\frac{1}{v}$ varying portion $\frac{g\sigma_o v_o}{v}$ and the excess over this part.

Then $$\Sigma = 2\, g\sigma_o v_o \int_{\sqrt{2\mu kT}}^{\infty} \frac{dv}{v^2} + \Sigma' ,$$ reduced resonance integral

so that $$R_e = \frac{4\, n_M\, v_T}{\sqrt{\pi}}\, \beta \left[\frac{g\sigma_o v_o}{2\mu kT} + \frac{\Sigma'}{2} \right] ,$$

and $$\hat{\sigma}_e = \frac{R_e}{n_e v_o} = g\sigma_o + \Sigma' \sqrt{\frac{\mu T}{4 T_o}} .$$

The total effective cross section can then be obtained from a consideration of the whole spectrum reaction rate:

$$\hat{\sigma} = \frac{\hat{\sigma}_M \phi_M + \hat{\sigma}_e \phi_e}{\phi_M + \phi_e}$$

$$= \frac{\hat{\sigma}_M + \hat{\sigma}_e\, b\beta}{1 + b\beta}$$

$$= g\sigma_o + \frac{\beta}{1+b\beta}\, \Sigma' \sqrt{\frac{4T}{\pi T_o}} .$$

If the reduced resonance integral Σ' ($\frac{1}{v}$ term subtracted) is normalised to the 2200 m/sec cross section by writing

$$s = \frac{\Sigma'}{\sigma_o} \sqrt{\frac{4T}{\pi T_o}} ,$$

and $\frac{\beta}{1+b\beta}$ is denoted by r,

then $$\hat{\sigma} = \sigma_o (g + rs) ,$$

where g(T) and s(T) are properties of the material and r characterises the epithermal neutron density.

Using this result the neutron density distribution function may be written:

$$n(v) = \frac{4n}{\sqrt{\pi}} \left\{ \frac{v^2}{v_T^3} \left[\exp - \left(\frac{v}{v_T} \right)^2 \right] (1-br) + \frac{r v_T}{v^2} \Delta \right\} , \qquad (3)$$

since $$1-br = \frac{1}{1+b\beta} = \frac{n_M}{n_e + n_M} = \frac{n_M}{n} .$$

Then the epithermal flux per unit lethargy $= n \bar{v} r$, and $r = \frac{(1-br) \times \text{flux/unit lethargy}}{n_M \bar{v}}$.

3.1 The Function Δ

The nature of the joining function is now considered in more detail. In the above discussion it was assumed that a sharp cut-off at μkT terminated the epithermal flux distribution. Such a cut-off will lead to a discontinuity in the total flux in the region where it is applied and joining functions have been proposed to eliminate this. The shape of these functions has been suggested by time-of-flight measurements after subtraction of the Maxwellian component.

The epithermal neutron density has been represented by

$$n_e = \frac{4 n_M}{\sqrt{\pi}} \beta \int_o^\infty \frac{v_T}{v^2} . \Delta . dv ,$$

and since β has been defined as $\frac{n_e}{b n_M}$,

then $$b = \frac{4}{\sqrt{\pi}} \int_o^\infty \frac{v_T}{v^2} . \Delta . dv ,$$

and the value of b will depend on the chosen form of Δ. Whatever function is used it is still possible to define an equivalent sharp cut-off by equating the neutron density in the sharp cut-off distribution to that with a more gradual cut-off.

Then $$\int_o^\infty \frac{v_T}{v^2} . \Delta . dv = \int_{\sqrt{2\mu kT}}^\infty \frac{v_T}{v^2} dv ,$$

giving

$$b = \frac{4}{\sqrt{\pi \mu}} .$$

Thus b defines the equivalent sharp cut-off for the particular joining function used. Westcott lists four alternative forms of joining function, of which Δ_4 is recommended as having the best experimental evidence in its favour. This function is shown in Figure 2 and contains an excess of neutrons over $\frac{1}{E}$ dependence in the joining region. In calculating resonance integrals of nuclei which show non-$\frac{1}{v}$ behaviour in the joining region, it is therefore not permissible to use the equivalent sharp cut-off μkT since this is obtained by conserving neutron density and not reaction rate. Providing the lowest energy resonance lies above about 2 eV however this difference will not be important.

4. CADMIUM RATIO ANALYSIS

The neutron density distribution is assumed to take the form:

$$n(v) = \frac{4}{\sqrt{\pi}}\, n \left\{ \frac{v^2}{v_T^3} \left[\exp - \left(\frac{v}{v_T} \right)^2 \right] (1-br) + \frac{r\, v_T}{v^2}\, \Delta_4 \right\},$$

where n = total neutron density

$$b = \frac{4}{\sqrt{\pi}} \int_0^\infty \frac{v_T}{v^2} \cdot \Delta_4 \cdot dv = \frac{4}{\sqrt{\pi}\,\mu}$$ and defines

an equivalent sharp cut-off at μkT to the epithermal spectrum

$$r = \frac{\beta}{1+b\beta}$$ where $b\beta = \frac{n_e}{n_M}$ and $n_e + n_M = n$

Δ_4 = describes the shape of the epithermal spectrum after subtraction of the Maxwellian component.

With a reactor spectrum of the above form Westcott has shown that the effective cross section can be written:

$$\hat{\sigma} = \sigma_o (g + rs) \quad ,$$

so that the per nucleus reaction rate of a bare foil can be written:

$$R_b = n v_o \sigma_o (g + rs) \quad ,$$

where $n v_o$ is the 'conventional' 2200 m/sec flux.

If it is assumed that cadmium transmits all neutrons of energy greater than E_{cd} and absorbs all neutrons of energy less than this the epicadmium reaction rate can be written:

$$R_e = \frac{4nr}{\sqrt{\pi}} \int_{\sqrt{2E_{cd}}}^\infty \frac{v_T}{v^2} \cdot \Delta_4 \cdot \sigma(v) \cdot v \cdot dv \quad . \tag{4}$$

Cadmium, however, is not a perfectly sharp filter of neutrons and it is necessary to frame some definition of an effective cut-off energy. This is usually done by conserving reaction rate between a cadmium covered foil and a hypothetical filter with sharp cut-off at E_{cd}, that is,

$$\int_0^\infty \Delta_{cd} \frac{\sigma(v)}{v}\, dv = \int_{\sqrt{2E_{cd}}}^\infty \frac{\sigma(v)}{v}\, dv \quad ,$$

where Δ_{cd} describes the spectrum shape after transmission through the cadmium and can be derived from consideration of the variation with energy of the cross sections of the cadmium and the detecting foil.

For $\frac{1}{v}$ cross section in the cut-off region (0.1 – 2 eV):

$$\int_0^\infty \Delta_{cd} \frac{dv}{v^2} = \frac{1}{\sqrt{2E_{cd}}} \quad .$$

Westcott has performed the calculation and defined a factor K by:

$$\int_0^\infty \Delta_{cd} \frac{dv}{v^2} = \frac{1}{\sqrt{2E_{cd}}} = \frac{1}{K} \sqrt{\frac{\pi}{32E_o}} \quad , \tag{5}$$

where K is a function of cadmium filter thickness and incident flux geometry and is proportional to the ratio of the neutron density in the transmitted spectrum to that in the incident spectrum. This can be seen from the following consideration:

The neutron density in the epithermal spectrum is:

$$n_e = \int_0^\infty \frac{4}{\sqrt{\pi}} \, n r \, \frac{v_T}{v^2} \, \Delta_4 \, dv = b n r \, .$$

The neutron density in the spectrum transmitted through cadmium is:

$$n'_e = \int_0^\infty \frac{4}{\sqrt{\pi}} \, n r \, \frac{v_T}{v^2} \, \Delta_{cd} \, dv = b' n r \, .$$

Thus $$\frac{n'_e}{n_e} = \frac{b'}{b} = \sqrt{\pi \mu} \sqrt{\frac{E_T}{\pi E_{cd}}} = \frac{4}{b} \sqrt{\frac{E_T}{\pi E_{cd}}}$$

and $$\frac{1}{K} = 4 \sqrt{\frac{E_o}{\pi E_{cd}}} = b \sqrt{\frac{T_o}{T}} \, \frac{n'_e}{n_e} \, .$$

With the present availability of digital computers and good cross section data there appears to be little difficulty in defining effective filter cut–offs by the above means. Stoughten and Halperin (1962) have published a compilation of such cut–offs for $\frac{1}{v}$ detectors shielded by B, Cd, Gd and Sm filters and their results for Cd are in reasonable agreement with those of Westcott. Further reference can be found in Dayton and Pettus (1957) and Gavin (1958). Unfortunately the consistency of the results of these calculations depends on a uniform assumption as to the form of the spectrum in the cut–off region, which is most difficult to measure unless recourse is made to beam time–of–flight measurements. In general, the exact location of the cadmium cut–off is not important for detectors with resonances well removed from the cut–off region although for purely $\frac{1}{v}$ detectors the assignment of a value for E_{cd} will bear greatly on the predicted sub–cadmium reaction rate.

Returning to Equation 4, the case where part of the non $\frac{1}{v}$ resonance integral lies below μkT must be considered. The argument is restricted to the case where this contribution is small, that is, where the first resonance lies above about 1 eV. Thus although the cross–section is non $\frac{1}{v}$ in the cut–off region the departure from the law is not great and the value of effective cut–off is assumed to be not greatly different from that for a $\frac{1}{v}$ detector.

The integral term of Equation 4 can be written:

$$\int_{\sqrt{2E_{cd}}}^{\infty} = \int_{\sqrt{2\mu kT}}^{\infty} - \int_{\sqrt{2\mu kT}}^{\sqrt{2E_{cd}}} \, ,$$

and the last integral in this equation can be written:

$$\int_{\sqrt{2\mu kT}}^{\sqrt{2E_{cd}}} = \frac{1}{v} \text{ component } + \text{ excess over } \frac{1}{v} \text{ component}$$

$$= - \left\{ \frac{g \sigma_o v_o}{\sqrt{2E_{cd}}} - \frac{g \sigma_o v_o}{\sqrt{2\mu kT}} \right\} + \frac{\delta \Sigma'}{2} \, ,$$

where $\delta\Sigma'$ is the contribution to Σ', the excess over $\frac{1}{v}$ resonance integral between μkT and E_{cd}, assuming $\Delta = 1$ for $E > \mu kT$.

$$\left. \begin{aligned} \text{Writing } W &= \frac{\delta \Sigma'}{\Sigma'} \, \frac{s_o}{g} \, , \\ \text{where } s_o &= s \sqrt{\frac{T_o}{T}} \, , \end{aligned} \right\}$$

then

$$\int_{\sqrt{2\mu kT}}^{\sqrt{2E_{cd}}} \sigma(v)\frac{dv}{v} = \frac{g\sigma_o v_o}{\sqrt{2E_{cd}}} - \frac{g\sigma_o v_o}{\sqrt{2\mu kT}} + \frac{\mathbb{W} g \sigma_o \sqrt{\pi}}{4} .$$

The epicadmium reaction rate is then

$$R_e = \frac{4nr v_T \sigma_o}{\sqrt{\pi}} \left\{ \frac{s}{4}\sqrt{\frac{\pi T_o}{T}} + \frac{g v_o}{\sqrt{2E_{cd}}} - \frac{\mathbb{W} g \sqrt{\pi}}{4} \right\} ,$$

and the cadmium ratio

$$R_{cd} = \frac{R_b}{R_e} = \frac{g + rs}{4r\sqrt{\frac{T}{T_o}} \left\{ \frac{s}{4}\sqrt{\frac{T_o}{T}} + \frac{g v_o}{\sqrt{2\pi E_{cd}}} - \frac{\mathbb{W} g}{4} \right\}}$$

$$= \frac{g + rs}{r\sqrt{\frac{T}{T_o}} \left\{ s\sqrt{\frac{T_o}{T}} + 4g\sqrt{\frac{E_o}{\pi E_{cd}}} - \mathbb{W} g \right\}} .$$

For a $\frac{1}{v}$ absorber, $s = \mathbb{W} = 0$ and $g = 1$,

so that

$$R_{cd} = \frac{1}{4r\sqrt{\frac{E_T}{\pi E_{cd}}}} = \frac{K}{r\sqrt{\frac{T}{T_o}}} ,$$

from Equation 5.

Hence for non-$\frac{1}{v}$ cross section between μkT and E_{cd} (assuming the same cut-off for both components):

$$R_{cd} = \frac{g + rs}{r\sqrt{\frac{T}{T_o}} \left\{ s_o + g\left(\frac{1}{K} - \mathbb{W}\right) \right\}} .$$

This equation must be further modified by taking into account the attenuation of resonance energy neutrons by the cadmium filter. To do this the denominator term s_o is reduced by the factor F. In addition, resonance self shielding by either large scattering or absorbing resonances will reduce the value of s in both numerator and denominator by the factor G_r, so that

$$R_{cd} = \frac{g + rs\,G_r}{r\sqrt{\frac{T}{T_o}} \left\{ s_o F G_r + g\left(\frac{1}{K} - \mathbb{W}\right) \right\}} .$$

If the thermal cross section is large, or the detector thick, appreciable flux distortion will occur with the introduction of the detector, increasing the apparent value of $r\sqrt{\frac{T}{T_o}}$ by the factor $\frac{1}{G_{th}}$. The corrected value of the epithermal index $r\sqrt{\frac{T}{T_o}}$ is then given by:

$$r\sqrt{\frac{T}{T_o}} = \frac{G_{th}}{(FR_{cd} - 1)\frac{s_o G_r}{g} + R_{cd}\left(\frac{1}{K} - \mathbb{W}\right)} . \qquad (6)$$

5. DERIVATION OF PARAMETERS

The use of Equation 6 to determine $r\sqrt{\frac{T}{T_o}}$ necessitates accurate knowledge of seven parameters apart from the cadmium ratio itself. The accuracy of the method is limited, not by the degree of precision

with which it is possible to measure R_{cd}, but by uncertainties in the values of G_r, G_{th}, s_o, F, W, g, and K. For this reason it does not appear worthwhile to attempt measurements of R_{cd} to better than about 1 per cent., since the error on the best resonance integral data is 3 per cent. and in most cases is much more than this.

5.1 Resonance Integral Data

From the definition above (Section 4):

$$s_o = \frac{2}{\sqrt{\pi}} \frac{\Sigma'}{\sigma_o}$$

where Σ' is the reduced resonance integral from μkT and σ_o is the 2200 m/sec value of the cross section. Both these quantities can be calculated if the resonance parameters are well known. The calculated values discussed below have been obtained using the resonance parameters listed in BNL 325 (Hughes and Swartz 1958) and supplement (1960).

Measured resonance integrals are usually referred to either a boron ($\frac{1}{v}$) standard or to a secondary standard whose resonance integral is well known. Unfortunately there have been few precise measurements of resonance activation integrals where the form of the epithermal spectrum has been checked by time-of-flight techniques. The only such measurements to our knowledge are those of Jirlow and Johannsson (1960) and Dahlberg et al. (1961). Where possible we have preferred to obtain our values of s_o using values of Σ' reported by these authors and values of σ_o from BNL 325 except where a more precise measurement is available in the literature since 1960.

◆ Au 197

Σ' (calculated) = 1566 barns

Σ' (measured) = 1490 ± 40 barns (Jirlow and Johansson, 1960)

σ_o (measured) = 98.8 ± 0.3 barns (BNL 325)

The measured and calculated resonance integrals are in good agreement. Using the experimental results,

$$s_o = 17.0 \pm 0.5 \quad ,$$

a result identical with the 'best value' reported by Bigham et al. (1961).

◆ In 115

This nuclide does not lead to a single radio-isotope upon neutron capture. For practical purposes, the 54 minute activity is of interest. Unfortunately the branching ratios of the resonances above 1.4 eV are not known. Assuming them to be the same as the main resonance at 1.4 eV the total resonance integral has been calculated as

Σ' (calculated) = 3083 barns.

Using the value for the total activation cross section of 189 ± 2 barns reported by Walker (1960),

$$s_o = 18.4 \pm 0.5 \quad .$$

Klopp and Zagotta (1962) report a calculated value of the resonance integral (including $\frac{1}{v}$ term) of 2525 barns in close agreement with the value obtained by Jacks (1961) of 2560 ± 130 barns for the 54 minute activation. Using the value 155 ± 10 barns reported in BNL 325 for the cross section for the 54 minute activation,

$$s_o = 18.2 \pm 1.5 \quad .$$

Bigham et al. (1961) quote for their best value

$$s_o = 18.8 \pm 0.5 \quad .$$

In this report we have adopted 18.5 ± 0.5 as the value of s_o for Indium.

◆ W 186

Few measurements are reported for this nuclide. Our calculated value is Σ' = 456 barns. Jacks (1961) reports a measured value of Σ = 396 ± 59 barns relative to Σ'(Au) of 1513 barns.

Chidley et al. (1962) report a measurement of $G_r s_o$ for W186; correcting this result for self shielding in the resonance at 18.8 eV and assuming a value of σ_o = 40 ± 5 barns (Lyon, 1960) a value of Σ' = 376 barns is obtained which is in good agreement with the value obtained by Jacks (Σ' = 379 barns). Using these experimental results,

$$s_o = 10.7 \pm 1.0 .$$

◆ Mn 55

Our calculated value is Σ' = 10.0 barns.

Many measurements are reported in the literature, but uncertainties in the degree of self shielding in the predominantly scattering resonances at 337 and 1080 eV appear to have been a source of error. A paper by Selander (1960) provides a means of correcting for this effect. This has been used by Dahlberg et al. (1961) in correcting their results. Their quoted value of Σ' = 8.15 ± 0.6 barns is in good agreement with the detailed work of Jacks (1961) and this value used in conjunction with σ_o = 13.2 ± 0.2 barns gives

$$s_o = 0.70 \pm 0.06 .$$

◆ Mo 100

Insufficient resonance data was available to calculate the resonance integral. The following values reported by Cabell (1960):

$$\Sigma = 3.73 \pm 0.2 \text{ barns}$$

$$\sigma_o = 0.199 \pm 0.005 \text{ barns} ,$$

give

$$s_o = 20.5 \pm 1 .$$

◆ Pt 198

No values of the resonance integral have been reported in the literature. The results of our measurements with the other detectors have been used to obtain values of $G_r s_o$ for Pt wire detectors. (Table 8).

◆ Cu 63

The calculated value of Σ' is 2.153 barns, in poor agreement with the measured value of 3.09 ± 0.15 barns reported by Dahlberg et al. (1961). The latter value has been preferred, and with a value of σ_o = 4.5 ± 0.15 barns gives

$$s_o = 0.77 \pm 0.05 .$$

5.2 Resonance Self Shielding

We have used the approach of Roe (1954) to evaluate self shielding factors for predominantly absorbing resonances and that of Selander (1960) for scattering resonances.

Table 9 summarises the contribution of the main resonance to the value of the reduced resonance integral of the detectors used in this work.

Unless very thick foils are used it will only be necessary to apply self shielding corrections to these main contributing resonances. The further the main resonance contribution decreases because of self shielding, the more important becomes the contribution of higher and unresolved resonances, the magnitude of which is difficult to calculate. We have defined the self shielding factor as used here by:

$$G_r = \frac{f_1 \Sigma_1' + \Sigma_{rest}'}{\Sigma'} \quad ,$$

where f_1 is the self shielding factor applied to the main resonance and calculated by the method of Roe (1954)

Σ_1' is the resonance integral contribution of the main resonance

Σ_{rest}' is the resonance integral contribution of higher and unresolved resonances

Σ' is the infinitely dilute reduced resonance integral = $\Sigma_1' + \Sigma_{rest}'$.

For Au 197 it has been assumed Σ_{rest}' = 50 barns

In 115 it has been assumed Σ_{rest}' = 125 barns

W 186 it has been assumed Σ_{rest} = 12 barns.

The variation of G_r with foil thickness as calculated above is shown in Figures 3 to 6. Some experimental verification has been obtained for indium and gold by analysing the cadmium ratio data of Jacks (1961) and Fastrup (1960). The agreement for gold is good, while for indium the experimental points lie below the calculated curve. Unfortunately in neither case is the method of comparison exact enough to enable a strong conclusion to be drawn. Better agreement would be obtained for indium if Σ_{rest}' was considerably less than 125 barns. In the case of W186, the resonance at 18.8 eV has a large scattering component which has been ignored in the calculation of the self shielding factor.

In all calculations involving the above three materials the calculated self shielding factors were used. For Mn55 the results of Selander (1960) were used, only the resonance at 337 eV being treated. In the case of Cu 63 self shielding factors (Figure 7) were roughly estimated using published effective resonance integrals by Bennett (1959). The results of cadmium ratio measurements with Mo 100 indicate that self shielding effects were negligible for the thicknesses used, and G_r was assumed to equal unity.

5.3 Thermal Flux Depression

The introduction of an absorbing foil into the region of neutron flux will cause a local flux depression in the foil and a perturbation of the flux in the surrounding moderator. The factor G_{th} to correct for this effect has been obtained from the work of Dalton and Osborne (1961). Their calculated values are in good agreement with the experimental results of Martinez (1961). Values of G_{th} as a function of foil thickness are shown in Figures 8 to 10.

5.4 Attenuation of Resonance Energy Neutrons by Cadmium

The factor F has been obtained from the results of Tittle (1951a, 1951b). The effect is only important for indium in the work reported here. For gold and all other detectors discussed, F has been assumed to equal unity.

5.5 Resonance Activation Below the Cadmium Cut-off

A difficulty arises in cases where an appreciable part of the resonance activation lies below E_{cd}. This is a consequence of splitting the resonance integral into a $\frac{1}{v}$ component and a resonance component.

It has been seen that no difficulty arises in defining an equivalent sharp cut-off to the cadmium transmission when the cross section obeys the $\frac{1}{v}$ law in the cut-off region; if on the other hand the cross section deviates from this law due to a low energy resonance, the cut-off for the two components will be different, and the lower limit of Σ' as defined by a cadmium cut-off will depend on the shape of the cross section in the cut-off region. This may be seen by writing

$$\int_0^\infty \Delta_{cd}\ \sigma'(v)\ \frac{dv}{v} = \int_{\sqrt{2E_{cd}'}}^\infty \sigma'(v)\ \frac{dv}{v} \quad ,$$

where $\sigma'(v)$ is the non-$\frac{1}{v}$ cross section and E'_{cd} is the effective cut-off energy. In this situation the usual definition of a resonance integral is incompatible with any attempt to define an effective cut-off energy for practical neutron filters.

An estimate of the resonance activation lost below the $\frac{1}{v}$ cut-off can be obtained if the departure from $\frac{1}{v}$ behaviour is not great and the same cut-off is assumed to hold for both components of the resonance integral. As shown by Bigham et al. the correction term W can then be written:

$$W = \frac{2}{\sqrt{\pi}} \frac{\Gamma_\gamma}{E_r} \sqrt{\frac{E_{cd}}{E_r}} \frac{s_o}{g} ,$$

where E_r is the energy of the lowest energy resonance and E_{cd} is the assumed cut-off. Thus W is not unduly sensitive to the value assumed for E_{cd}.

6. REACTION RATE RATIO ANALYSIS

The ratio of the reaction rates of two nuclides irradiated simultaneously in a well moderated spectrum may be simply expressed in terms of the Westcott parameters by:

$$R_r = \frac{\sigma_{ox} \{ g_x (T_1) + r \frac{G_{rx}}{G_{th}} s_x (T_1) \}}{\sigma_{oy} \{ g_y (T_1) + r \frac{G_{ry}}{G_{th}} s_y (T_1) \}} ,$$

where G_{th} is the flux depression factor for the composite foil and it is assumed no effect arises from resonance self shielding of one component by another. This may be avoided by choosing nuclide y (say) to be free of major resonances and diluting the resonance detector x in it so as to minimise self shielding effects.

If the absolute counter efficiencies for the two activities are not known the ratio may be normalised by irradiation in a thermal flux so that

$$R_{th} = \frac{\sigma_{ox} g_x (T_2)}{\sigma_{oy} g_y (T_2)} ,$$

then

$$R = \frac{R_r}{R_{th}} = \frac{g_x (T_1) g_y (T_2) + r \frac{G_{rx}}{G_{th}} s_x (T_1) g_y (T_2)}{g_x (T_2) \{ r \frac{G_{ry}}{G_{th}} s_y (T_1) + g_y (T_1) \}}$$

7. EXPERIMENTAL RESULTS

The numerical results are given in Tables 1 to 8.

7.1 Measurement of $r\sqrt{\frac{T}{T_o}}$

Values of the epithermal index were obtained from cadmium ratio measurements on the six detectors by means of Equation 6. Since these detectors are sensitive to different regions of the spectrum by virtue of the location of their major resonances, the consistency of the values of $r\sqrt{\frac{T}{T_o}}$ supports the assumption of a $\frac{1}{E}$ slowing down spectrum. Tables 1 to 6 show the data from which the the values of $r\sqrt{\frac{T}{T_o}}$ were deduced.

The mean values of $r\sqrt{\frac{T}{T_o}}$ for each detector are shown in Table 9.

7.2 Measurement of the Effective Neutron Temperature

It has been shown in section 3 that the function g(T) will be a sensitive measure of the neutron temperature if the cross section in the thermal region is markedly different from the $\frac{1}{v}$ shape and the neutron velocity distribution is a pure Maxwellian.

However, since neutron behaviour in an actual reactor includes processes such as leakage and absorption, the Maxwellian distribution will be distorted and g(T) will then define an effective neutron temperature, that is, the temperature of a Maxwellian which would give the same reaction rate as does the actual spectrum. As pointed out by Villemoes and Fastrap (1962) the two conditions which define the effective temperature are:

(i) The neutron density in the actual spectrum $n_a(v)$ is equal to the density in the assumed Maxwellian spectrum.

(ii) Reaction rate is conserved between the actual and the assumed spectrum, that is,

$$\int_0^\infty \left\{ n_a(v) - \frac{4}{\sqrt{\pi}} n_M \frac{v^2}{v_T^3} \left[\exp - \left(\frac{v}{v_T} \right)^2 \right] \right\} v \sigma(v) \, dv = 0 .$$

It can be seen that effective temperature defined in this manner depends upon the nature of the function $v\sigma(v)$ if the actual spectrum deviates from the Maxwellian shape. The concept of effective temperature is thus only useful where the departure from a Maxwellian distribution at low energies is not great.

The above discussion has restricted the argument to spectra with no contribution from slowing down sources. In order to utilize g(T) as a means of measuring the effective temperature of a reactor spectrum it is therefore necessary to find a way of removing the epithermal contribution from the total observed reaction rate. It has been shown that the case of resonance behaviour in the joining region presents difficulties if the Westcott approach is used. Providing the resonance parameters are well known the s factor may be calculated, though in this case it will be more sensitive to the form of joining function assumed.

However, if the epithermal contribution to the total reaction rate is small compared to the thermal reaction rate, it will not be necessary to specify the value of s with great precision in order to measure T. Moreover, if the major resonance lies below about 0.2 eV and the next resonance above about 2 eV, it will be possible to obtain an approximate value of the epicadmium resonance integral. The sub-cadmium contribution to s may then be calculated if the resonance parameters are well known and the shape of the spectrum in the joining region is assumed or is known. Such an approximation has been used by Hyder et al. (1961) to obtain an s value for Lu 176.

Since our future interest will lie with intermediate spectra, the concept of effective temperature does not appear to be a useful manner of specifying low energy reaction rates; for the sake of completeness however the effective temperature in the centre of the MOATA internal reflector has been measured by obtaining the Lu:Mn reaction rate ratio as described by Hyder et al., the ratio being normalised to that measured in the Low Flux Facility. A single measurement only was performed, the foil being prepared by thoroughly mixing the oxides of lutetium and manganese and pressing 30 mg of the mixture between two perspex discs. The complete foil contained 25 mg Lu_2O_3 and 5 mg of Mn_3O_4. The Mn activity was counted by biassing off the lower energy Lu activity, and after four days the Lu 177 activity was counted. The measured value of the reaction rate ratio normalised to that in the Low Flux Facility was 1.09 ± 0.02, corresponding to an effective neutron temperature of 45 ± 5 °C using the g and s_4 values listed in CRRP 960 (Westcott 1960).

7.3 Comparison of Observed and Calculated Reaction Rate Ratios

The foils used in this work were manufactured from Cu : In alloy, (5.01 ± 0.01) per cent. by weight In, and Cu : Au alloy (1.69 ± 0.04) per cent. by weight gold.

Normalizing irradiations were performed in the Low Flux Facility, and the reactor irradiation in the centre of the MOATA graphite reflector.

The calculated ratios assumed a reactor neutron spectrum characterised by:

$$r \sqrt{\frac{T}{T_o}} = 0.0389$$

$$T_1 = 45 \,^\circ C .$$

The normalizing thermal spectrum was assumed to be a pure Maxwellian of characteristic temperature

$$T_2 = 23\,^{\circ}C .$$

The measurements were repeated twice for each Cu : Au foil. Each foil was counted in two ways, firstly by counting both activities to a negligible level and secondly by using pulse height discrimination to separate the two activities. The same procedure was followed for the Cu : In foils but the irradiations were not repeated.

These measurements could be improved in precision but as the foils were not entirely satisfactory (being of uncertain area as a consequence of poor punching) further work was deferred until a new set of foils could be obtained.

Table 7 gives the numerical results of these measurements.

7.4 The Resonance Integral of Platinum 198

Using the mean value of the epithermal index (deduced from cadmium ratio measurements with the other six detectors) in conjunction with Equation 6, values of $G_r s_o$ for platinum wires of diameter 5, 10, and 20 mil have been obtained and these are shown in Table 8. The value of s_o has been estimated by fitting these results to a curve of the form

$$G_r = \sqrt{\frac{S}{S + A}} ,$$

giving $s_o = 14.9$. Assuming $\sigma_o = 4$ barns for Pt 198, the reduced resonance integral for this isotope is 53 barns.

8. DISCUSSION

Reaction rates of nuclei with resonances above about 10 eV can be used to obtain values of the epithermal index by cadmium ratio techniques with a precision limited by the accuracy of the cross section data. In such cases the correction term W is zero and the factor K can be calculated with good precision providing the thickness of cadmium used is sufficient to prevent thermal activations making the value of the effective cut-off dependent on the value of the epithermal index.

Unfortunately cross section data for several potentially useful detectors are not known accurately and it would appear worthwhile to attempt to obtain more precise values for the thermal cross section and resonance integrals of the detectors used in this work, excepting gold and indium. In assigning errors to the individual $r\sqrt{\frac{T}{T_o}}$ values quoted in this report, only errors in R_{Cd} and s_o have been considered since these contribute most to the total error.

The value of the reduced resonance integral for higher energy resonances is quite sensitive to the form of the epithermal spectrum. Values of Σ' for gold, manganese, and copper have been calculated, assuming a neutron flux distribution function given by $E^{\alpha-1}$, for values of α from zero to 0.05 in steps of 0.01. These values, normalised to the value of Σ' for $\alpha = 0$, are shown in Table 10. Using values of s_o appropriate to the spectrum characterised by $\alpha = 0.02$, the values of the epithermal index deduced from the gold, manganese, and copper cadmium ratios become 0.0373, 0.0373, and 0.0366 respectively. Although our measurements are not precise enough to draw a definite conclusion, there is some evidence that the epithermal spectrum is better characterised by the form $E^{-0.98}$ rather than E^{-1}. An alternative explanation for the increase in the value of the epithermal index with increasing energy of the principal resonance could be that there are relatively fewer neutrons in the lower energy region of the epithermal spectrum than suggested by Equation 3.

It appears probable to us that the values of s quoted by Westcott are too high in the case of gold and indium.

The use of indium as a detector is complicated by difficulties in defining the cadmium cut-off and the fractional loss of resonance activation due to the presence of the cadmium filter. Determination of the epithermal index by the reaction rate ratio avoids these difficulties, and it is unfortunate that the measured values of the reaction rate ratios have large errors associated with them. In order

to reduce these errors, it will be necessary to obtain absolutely uniform foils so that it is possible to perform the thermal irradiation simultaneously with the reactor irradiation. This will permit both foils to be counted alternately and thus avoid drifts in counter efficiency.

The analysis by Wall (1963) shows that the contribution to the total activation by the start up and shutdown periods of reactor operation is sensibly independent of the half life of the activity for half lives greater than a few minutes and reasonable irradiation times. Therefore it was not necessary to apply any correction for this effect to the measured reaction rate ratios. For the cadmium ratio measurements the conditions for the bare and cadmium covered irradiations were made as identical as possible in order to minimise the effect of the rate of rise to power and the rate of shutdown.

9. ACKNOWLEDGMENTS

The authors are indebted to Miss M. Daley for much of the numerical work. Mr. G. Doherty calculated all the resonance integrals quoted in this report as Σ (calc.).

10. REFERENCES

Bennett, R.A. (1959). – H.W. 63576.

Bigham, C.B., Chidley, B.G., and Turner, R.B. (1961). – AECL 1350.

Boldeman, J., Nicholson, K., and Rose, A. (1962). – AAEC/TM 164.

Cabell, M.J. (1960). – J. Nucl. Energy Pt. A 12 : 172–6.

Chidley, B.G., Turner, R.B., and Bigham, C.B. (1961). – AECL 1419.

Dahlberg, R., Jirlow, K., and Johansson, E. (1961). – Reactor Sci. and Tech. (J. Nucl. Energy Parts A and B) 14 : 53–54.

Dalton, G.R., and Osborne, R.K. (1961). – Nucl. Sci. and Eng. 9 (2) : 198–210.

Dayton, I.E., and Pettus, W.G. (1957). – Nucleonics 15 (12) : 86–88.

Fastrup, B. (1959). – RISO Report No. 11.

Gavin, G.B., and Stewart, H.B. (1959) . – Naval Reactor Physics Handbook Vol. III.

Hughes, D.J., and Schwartz, R.B. (1958). – BNL 325 (And Supplement).

Hyder, H.R.McK., Kenward, C.J., and Price, G.A. (1961). – AERE–M552.

Jacks, G.M. (1961). – DP 608.

Jirlow, K., and Johansson, E. (1960). – J. Nucl. Energy Part A 11 : 101–107.

Klopp, D.A., and Zagotta, W. F. (1962). – Trans. Am. Nucl. Soc. 5 : 377.

Lang, G., and Rose, A. – AAEC Internal Report RP/TN 32

Lyon, W.S. (1960). – Nucl. Sci. and Eng. 8 : 378–380.

Marks, A. (1962). – Atomic Energy 5 (4) : 9 – 21.

Martinez, J.S. (1961). – UCRL 6520.

Roe, G.M. (1954). – KAPL 1241.

Selander, W.N. (1960). – AECL 1077.

Stoughten, R.W., and Halperin, J. (1962). – ORNL–TM–236.

Tittle, C.W. (1951a). – Nucleonics 8 (6) : 5–9.

Tittle, C.W. (1951b). – Nucleonics 9 (1) : 60–7.

Villemoes, P., and Fastrup, B. (1962). – RISO Report No. 33.

Walker, W.H. (1960). – AECL 1054.

Wall, T. (1963). – AAEC Internal Report RPTN/31.

Westcott, C.H. (1956). – CRRP 680.

Westcott, C.H. (1958). – CRRP 787.

Westcott, C.H. (1960). – CRRP 960.

TABLE 1

VALUES OF $r\sqrt{\frac{T}{T_o}}$ DEDUCED FROM CADMIUM RATIOS WITH INDIUM

MATERIAL: NATURAL INDIUM **

DETECTOR: In 115

Alloy foils 5.5 ±0.1% Indium in Lead

s_o = 18.5 ±0.5

g = 1.021

Form	Surface Density	G_r	G_{th}	$\frac{1}{K}$	W	F	R_{cd}	$r\sqrt{\frac{T}{T_o}}$
Foil	10 μg cm^{-2}	1.0	1.0	0.436	0.410	0.930	2.655 ±0.03	0.0374 ±0.002
Foil	280 μg cm^{-2}	0.962	1.0	0.436	0.410	0.930	2.625 ±0.03	0.0396 ±0.002
Alloy Foil	5.7 mg cm^{-2}	0.640	0.974	0.436	0.410	0.91	3.387 ±0.04	0.0389 ±0.002
Alloy Foil	*	*	0.965	0.436	0.410	0.922	4.146 ±0.09	0.0382 ±0.003
Alloy Foil	27.0 mg cm^{-2}	0.362	0.925	0.436	0.410	0.91	5.075 ±0.04	0.0381 ±0.002

* The bare foil had a surface density of 10.26 mg cm^{-2}, the cadmium covered foil a surface density of 12.17 mg cm^{-2}. The values of G_r for these are 0.530 and 0.498 respectively.

** that is, natural isotopic composition.

TABLE 2

VALUES OF $r\sqrt{\frac{T}{T_o}}$ DEDUCED FROM CADMIUM RATIOS WITH GOLD

MATERIAL: NATURAL GOLD

DETECTOR: Au 197

Wire detectors all one cm long

$s_o = 17.0 \pm 0.5$

$g = 1.0056$

Form	Diameter or Surface Density	G_r	G_{th}	$\frac{1}{K}$	W	F	R_{cd}	$r\sqrt{\frac{T}{T_o}}$
Wire	0.001 in	0.480	0.984	0.494	0.092	1.0	3.940	0.0384
							±0.1	±0.002
Wire	0.005 in	0.248	0.942	0.494	0.092	1.0	6.05	0.0397
							±0.04	±0.001
Wire	0.0128 in	0.162	0.858	0.494	0.092	1.0	8.204	0.0371
							±0.09	±0.001
Foil	0.493 mg cm^{-2}	0.960	1.00	0.436	0.104	1.0	2.51	0.0393
							±0.02	±0.002
Foil	50 mg cm^{-2}	0.361	0.960	0.436	0.104	1.0	4.79	0.0388
							±0.07	±0.002

TABLE 3

VALUES OF $r\sqrt{\frac{T}{T_o}}$ DEDUCED FROM CADMIUM RATIOS WITH TUNGSTEN

MATERIAL: NATURAL TUNGSTEN

DETECTOR: W 186

Wire detectors all one cm long

$s_o = 10.7 \pm 1.0$

$g = 1.00$

Form	Diameter (in x 10^{-3})	G_r	G_{th}	$\frac{1}{K}$	W	F	R_{cd}	$r\sqrt{\frac{T}{T_o}}$
Wire	0.8	0.850	0.998	0.494	0	1.0	3.75 ±0.1	0.0373 ±0.005
Wire	5.0	0.532	0.987	0.494	0	1.0	5.16 ±0.08	0.0378 ±0.004
Wire	9.8	0.405	0.975	0.494	0	1.0	6.36 ±0.1	0.0371 ±0.004

TABLE 4

VALUES OF $r\sqrt{\frac{T}{T_o}}$ DEDUCED FROM CADMIUM RATIOS WITH MOLYBDENUM

MATERIAL: NATURAL MOLYBDENUM

DETECTOR: Mo 100

Wire detectors all one cm long

$s_o = 20.5 \pm 1$

$g = 1.00$

Form	Diameter or Thickness (in x 10^{-3})	G_r	G_{th}	$\frac{1}{K}$	W	F	R_{cd}	$r\sqrt{\frac{T}{T_o}}$
Foil	2	1.00	1.00	0.437	0	1.0	2.12 ±0.04	0.0420 ±0.004
Wire	5	1.00	1.00	0.494	0	1.0	2.18 ±0.07	0.0394 ±0.005
Wire	20	1.00	1.00	0.494	0	1.0	2.17 ±0.03	0.0399 ±0.004

TABLE 5

VALUES OF $r\sqrt{\frac{T}{T_o}}$ DEDUCED FROM CADMIUM RATIOS WITH MANGANESE

MATERIAL: NATURAL MANGANESE or Ni : Mn alloy

DETECTOR: Mn 55

Wire detector one cm long

$s_o = 0.70 \pm 0.06$

$g = 1.00$

Form	Diameter or Surface Density	G_r	G_{th}	$\frac{1}{K}$	W	F	R_{cd}	$r\sqrt{\frac{T}{T_o}}$
Foil	13.5 mg cm^{-2} 90% Mn 10% Ni	0.93	0.995	0.437	0	1	23.60 ±0.5	0.0398 ±0.002
Foil	10 μg cm^{-2}	1.00	1.00	0.437	0	1	21.96 ±0.2	0.0416 ±0.002
Wire	0.020 in * 90% Mn 10% Ni	0.60	0.955	0.494	0	1	26.98 ±0.4	–

* Value of G_r obtained from Equation 6 with $r\sqrt{\frac{T}{T_o}} = 0.040$

TABLE 6

VALUES OF $r\sqrt{\frac{T}{T_o}}$ DEDUCED FROM CADMIUM RATIOS WITH COPPER

MATERIAL: NATURAL COPPER

DETECTOR: Cu 63

$s_o = 0.77 \pm 0.05$

$g = 1.00$

Form	Thickness (in x 10^{-3})	G_r	G_{th}	$\frac{1}{K}$	W	F	R_{cd}	$r\sqrt{\frac{T}{T_o}}$
Foil	2	0.88	1.00	0.437	0	1.00	23.06 ±0.3	0.0399 ±0.002

TABLE 7

REACTION RATE RATIOS OF Cu : In AND Cu : Au ALLOY FOILS

COPPER : INDIUM ALLOY

Foil Thickness (in x 10^{-3})	Surface Density (In) (mg cm^{-2})	Surface Density (Cu) (mg cm^{-2})	R (Calculated)	R (Measured)
5	6.51	89.0	1.379	1.431 ±0.03
10	10.40	142.4	1.364	1.395 ±0.03
20	21.87	299.3	1.276	1.278 ±0.03

COPPER : GOLD ALLOY

Foil Thickness (in x 10^{-3})	Equivalent Gold Thickness (in x 10^{-3})	Surface density (Cu) (mg cm^{-2})	R (Calculated)	R (Measured)
2.5	0.02	40	1.554	1.539 ±0.06
5.0	0.04	81	1.537	1.531 ±0.06
10.0	0.08	160	1.491	1.464 ±0.03
20.0	0.16	330	1.415	1.414 ±0.05

TABLE 8

EFFECTIVE s_o VALUES FOR PLATINUM WIRES

Wire diameter (in x 10^{-3})	R_{cd}	$G_r s_o$	s_o
5	2.67 ± 0.03	13.81	14.90
10	2.76 ± 0.04	13.01	14.99
20	3.04 ± 0.07	11.56	14.88

TABLE 9

LOCATION OF PRINCIPAL RESONANCES FOR DETECTORS AND MEAN VALUES OF $r\sqrt{\frac{T}{T_o}}$ FROM THEIR CADMIUM RATIOS

Detector	Energy of main resonance (eV)	Contribution of main resonance to Σ'	Mean value $r\sqrt{\frac{T}{T_o}}$
In 115	1.457	96%	0.0384
Au 197	4.906	97%	0.0387
W 186	18.8	97%	0.0372
Pt 198	95	?	–
Mn 55	337	87%	0.0403
Mo 100	367	?	0.0404
Cu 63	580	78%	0.0399

TABLE 10

VARIATION OF THE REDUCED RESONANCE INTEGRAL WITH THE SLOPE OF THE EPITHERMAL FLUX DISTRIBUTION FUNCTION

α	0	0.01	0.02	0.03	0.04	0.05
Au 197	1.0	1.018	1.037	1.056	1.075	1.096
Mn 55	1.0	1.062	1.128	1.198	1.272	1.351
Cu 63	1.0	1.072	1.147	1.228	1.311	1.405

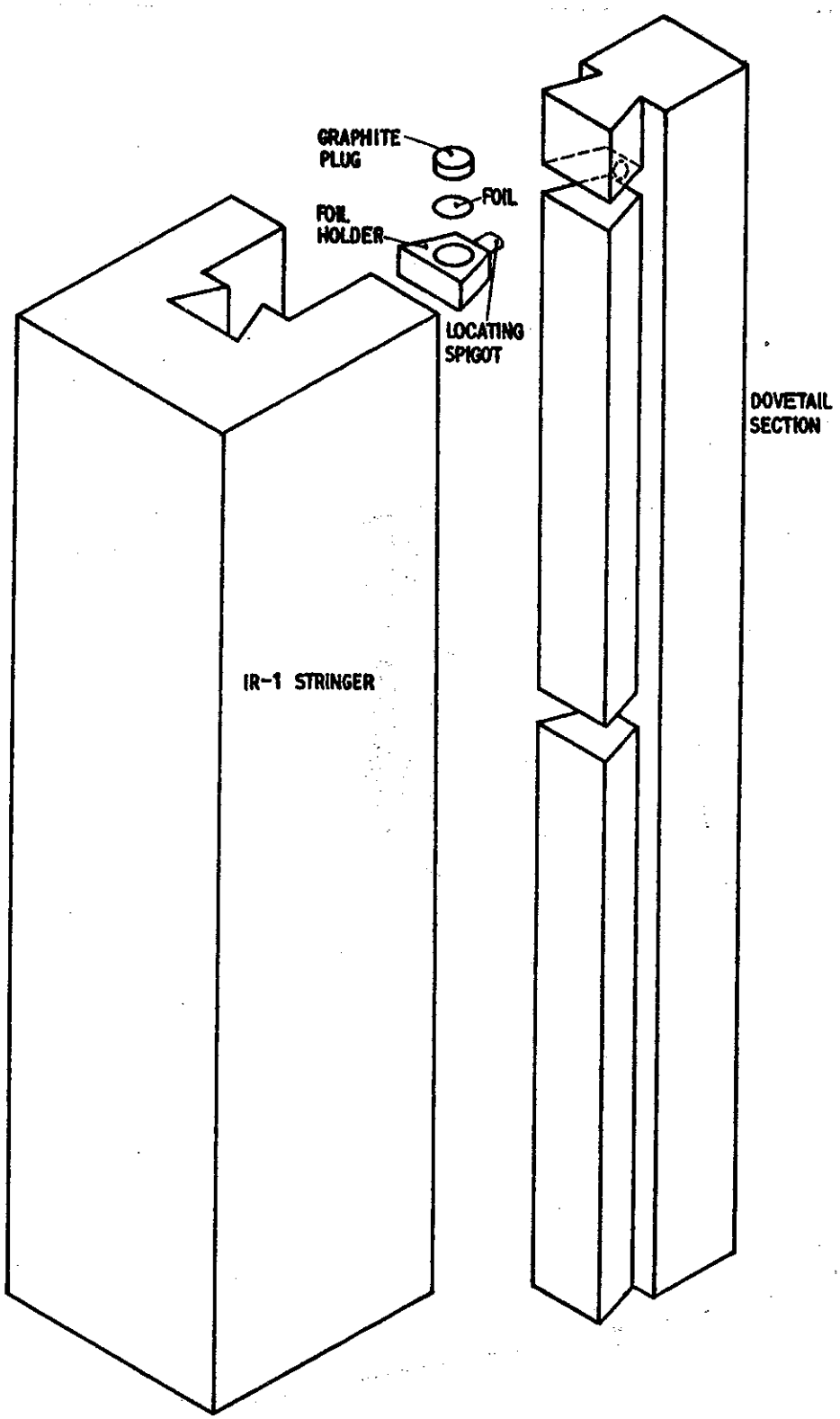

FIGURE 1 MOATA DOVETAIL STRINGER

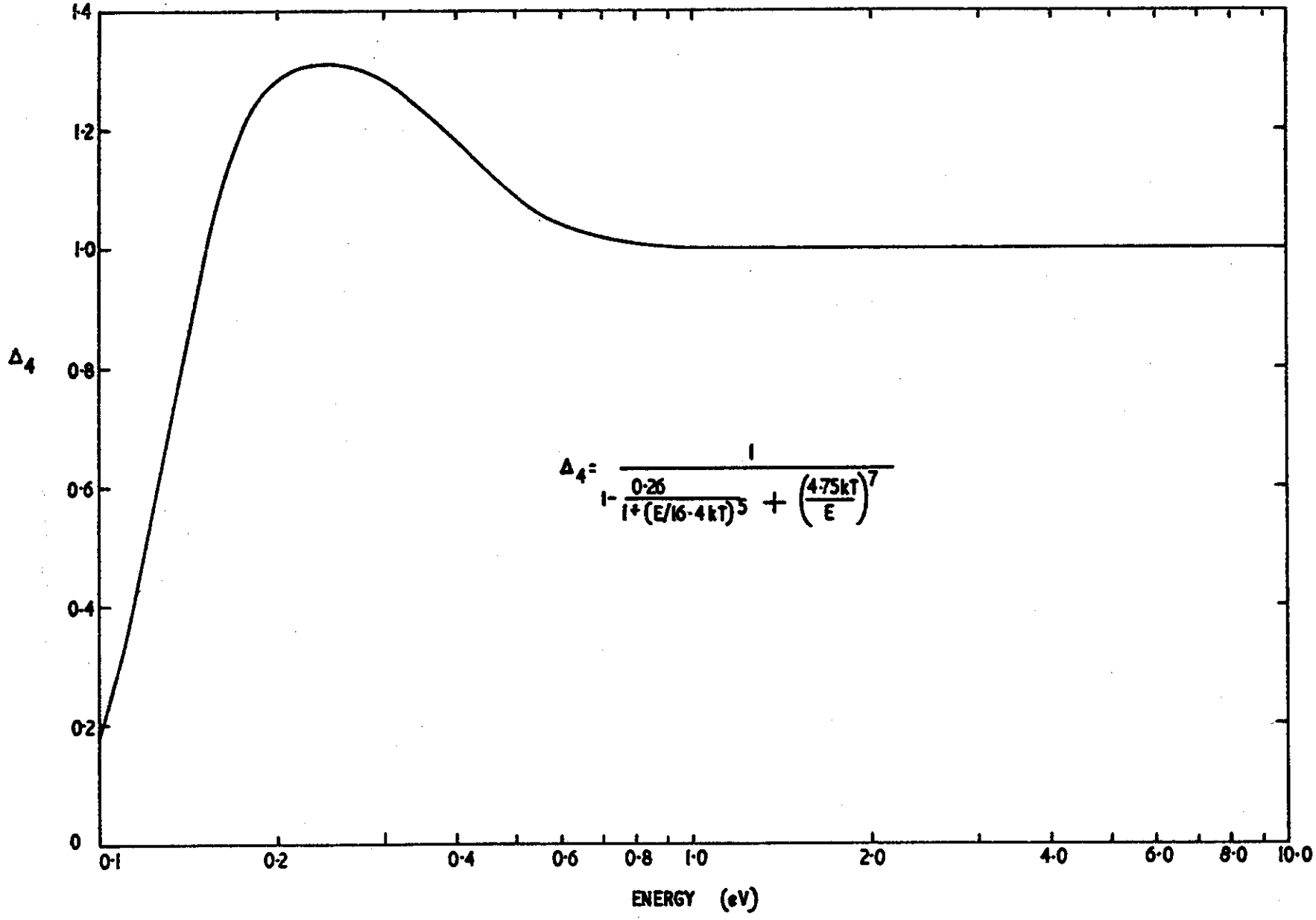

FIGURE 2 JOINING FUNCTION Δ_4

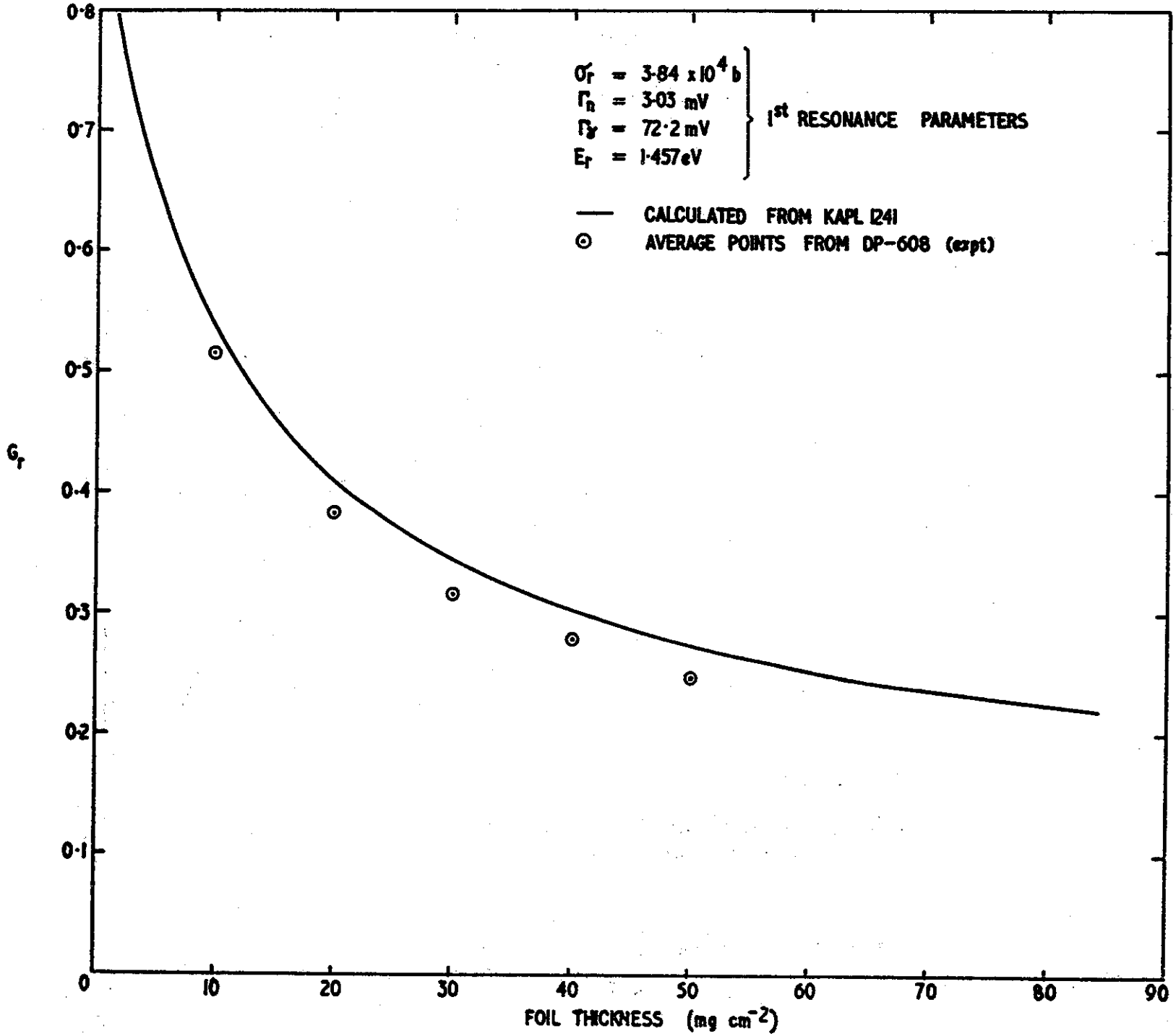

FIGURE 3 SELF SHIELDING FACTORS FOR In 115 SLABS

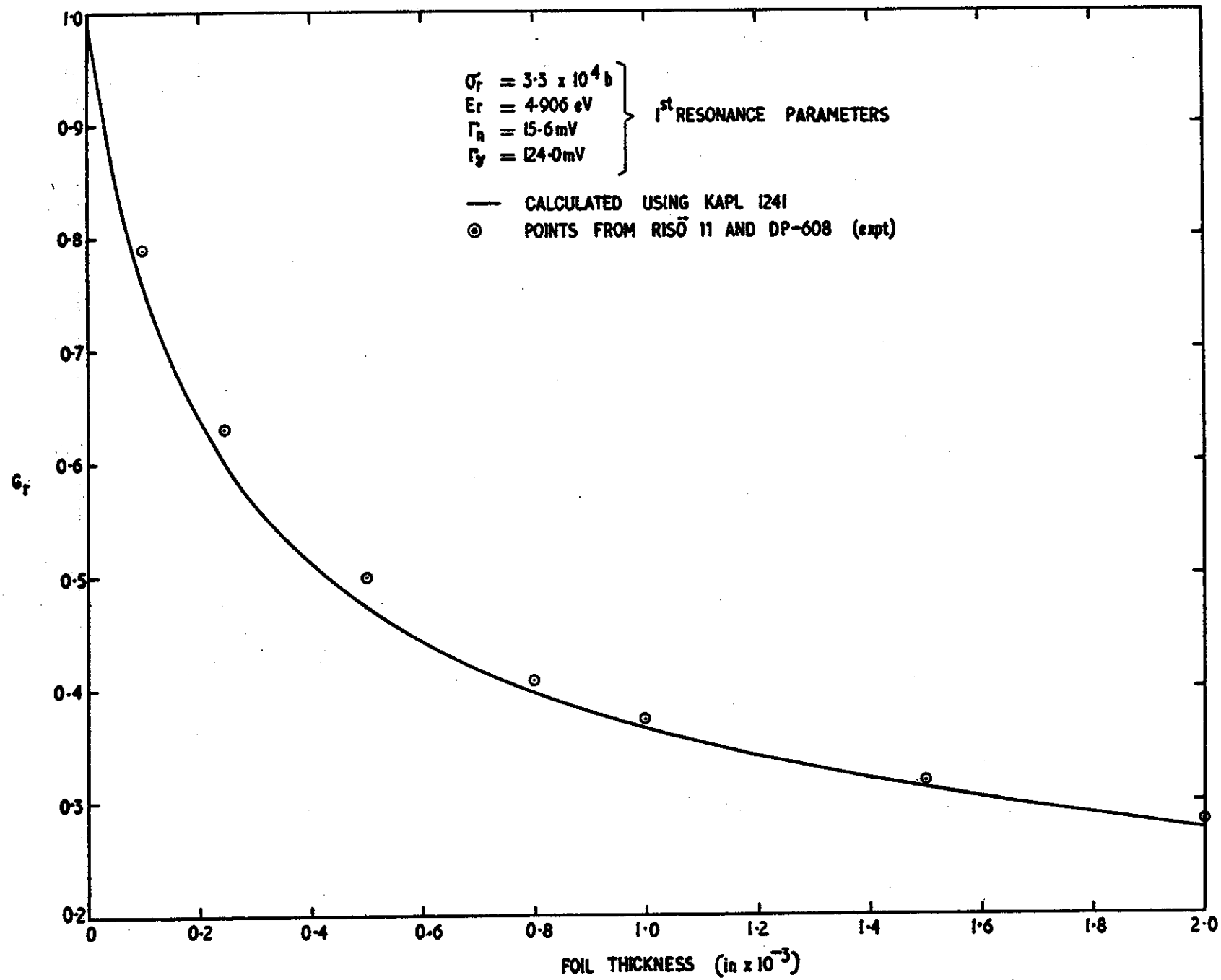

FIGURE 4 SELF SHIELDING FACTORS FOR Au197 SLABS

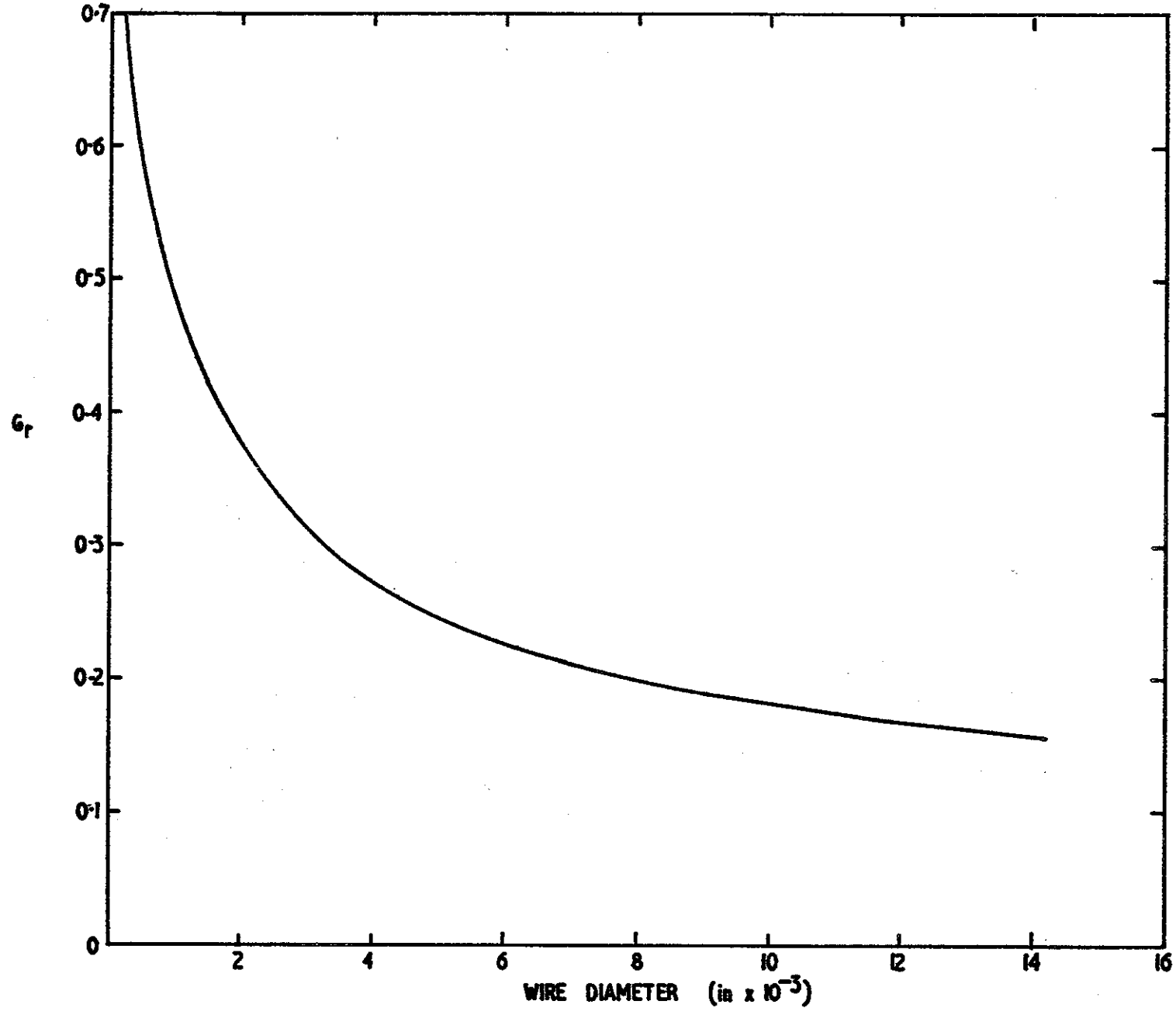

FIGURE 5 SELF SHIELDING FACTORS FOR Au 197 WIRES
(CALCULATED FROM KAPL 1241)

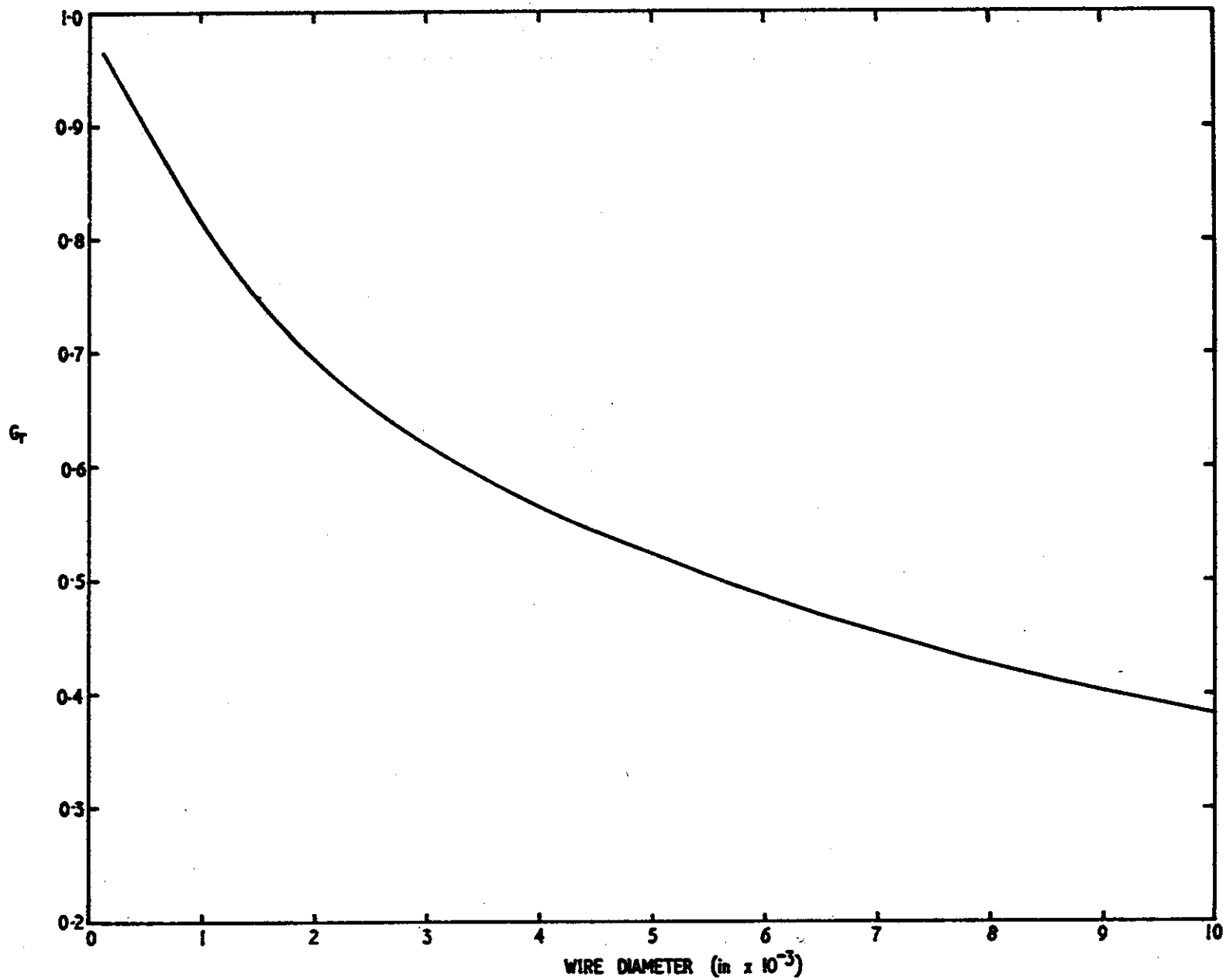

FIGURE 6 SELF SHIELDING FACTORS FOR W186 WIRES
(CALCULATED FROM KAPL 1241)

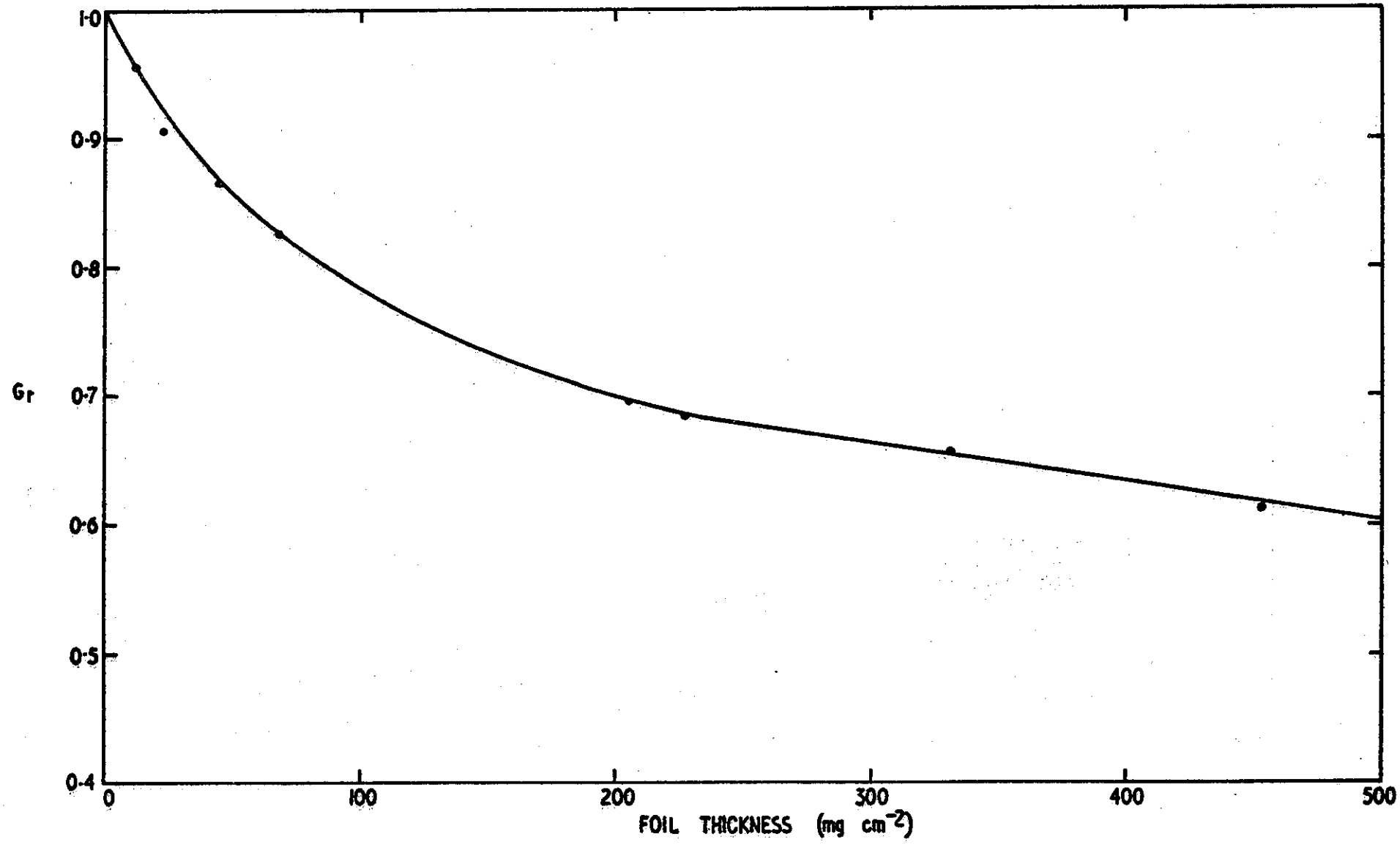

FIGURE 7 SELF SHIELDING FACTORS FOR Cu 63 SLABS

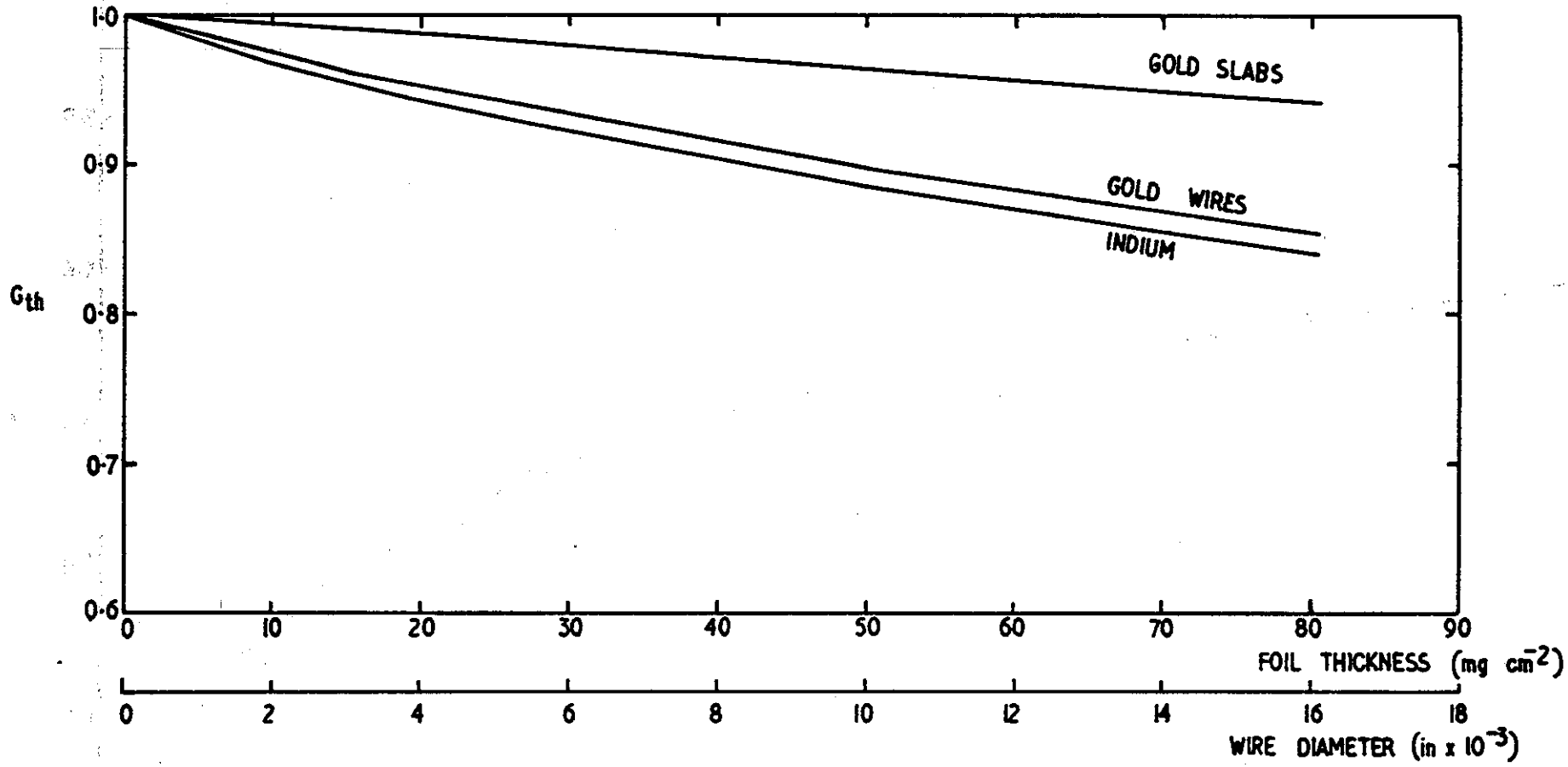

FIGURE 8 THERMAL FLUX DEPRESSION FACTORS FOR GOLD AND INDIUM

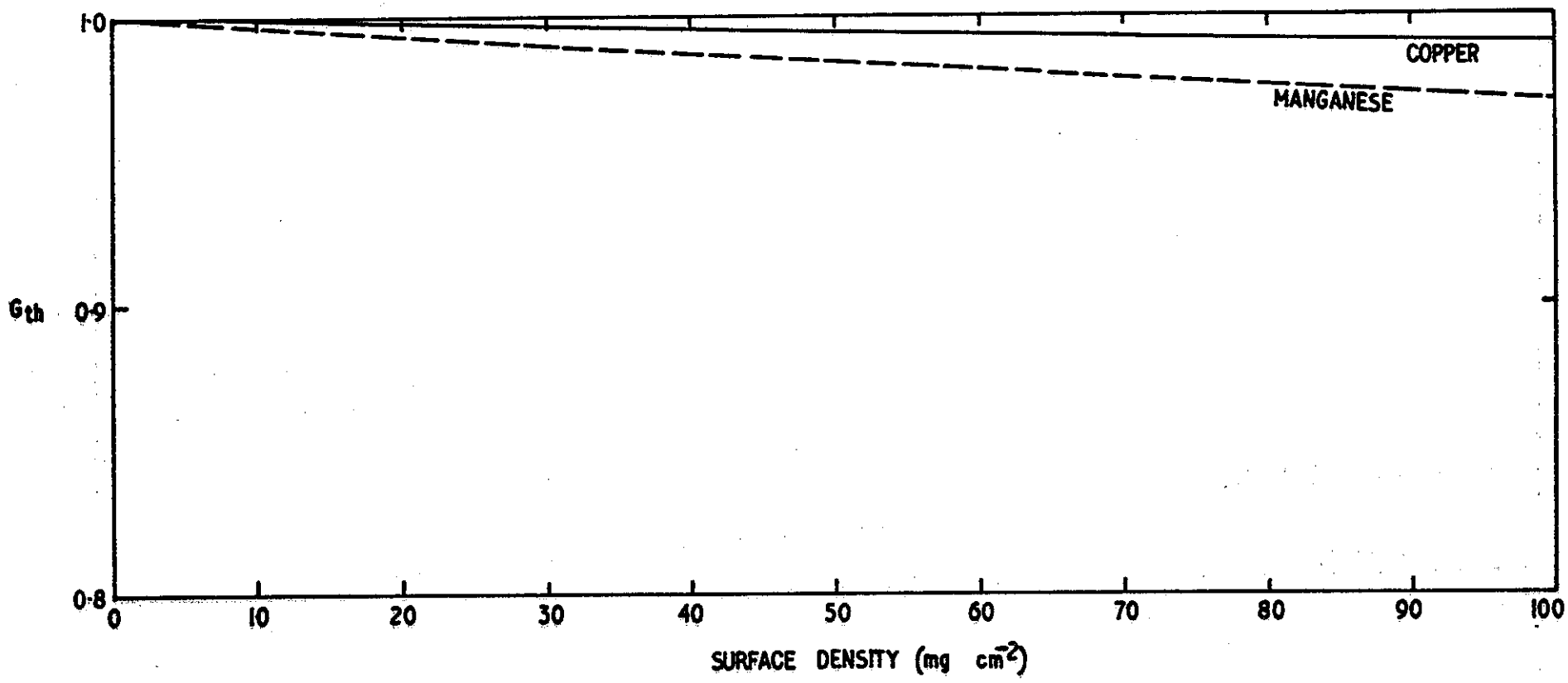

FIGURE 9 THERMAL FLUX DEPRESSION FACTORS FOR COPPER AND MANGANESE SLABS

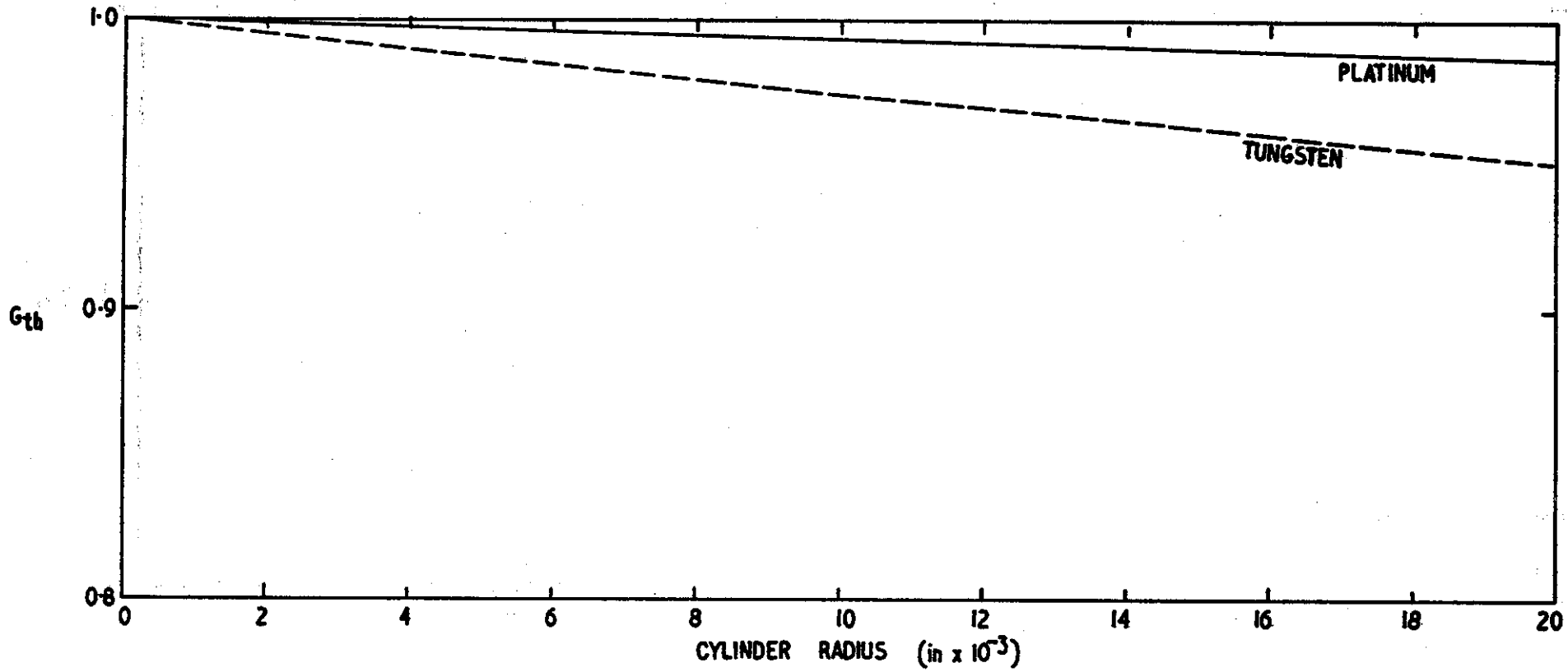

FIGURE 10 THERMAL FLUX DEPRESSION FOR PLATINUM AND TUNGSTEN CYLINDERS